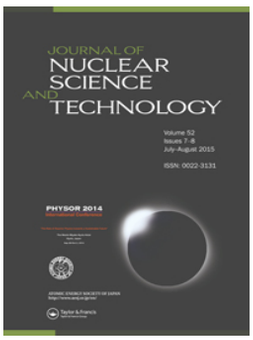

Journal of Nuclear Science and Technology

ISSN: 0022-3131 (Print) 1881-1248 (Online) Journal homepage: https://www.tandfonline.com/loi/tnst20

Experimental estimation of the delayed neutron fraction β_{eff} of the MAESTRO core in the MINERVE zero power reactor

Erez Gilad, Oleg Rivin, Hanania Ettedgui, Ilan Yaar, Benoit Geslot, Alexandra Pepino, Jacques Di Salvo, Adrien Gruel & Patrick Blaise

To cite this article: Erez Gilad, Oleg Rivin, Hanania Ettedgui, Ilan Yaar, Benoit Geslot, Alexandra Pepino, Jacques Di Salvo, Adrien Gruel & Patrick Blaise (2015) Experimental estimation of the delayed neutron fraction β_{eff} of the MAESTRO core in the MINERVE zero power reactor, Journal of Nuclear Science and Technology, 52:7-8, 1026-1033, DOI: 10.1080/00223131.2015.1038331

To link to this article: https://doi.org/10.1080/00223131.2015.1038331

Published online: 06 May 2015.

Journal of Nuclear Science and Technology, 2015
Vol. 52, Nos. 7–8, 1026–1033, http://dx.doi.org/10.1080/00223131.2015.1038331

Taylor & Francis
Taylor & Francis Group

ARTICLE

Physor 2014

Experimental estimation of the delayed neutron fraction β_{eff} of the MAESTRO core in the MINERVE zero power reactor

Erez Gilad[a]*, Oleg Rivin[b], Hanania Ettedgui[b], Ilan Yaar[b], Benoit Geslot[c], Alexandra Pepino[c], Jacques Di Salvo[c], Adrien Gruel[c] and Patrick Blaise[c]

[a]*The Unit of Nuclear Engineering, Ben-Gurion University of the Negev, Beer-Sheva 84105, Israel;* [b]*Department of Physics, Nuclear Research Center Negev, Beer-Sheva 84190, Israel;* [c]*Commissariat à l'ÉnergieAtomiqueet aux Énergies Alternatives, CEA DEN/CAD/DER/SPEx/LPE, Saint Paul-les-Durance 13108, France*

(*Received 22 January 2015; accepted final version for publication 1 April 2015*)

A method for determining the effective delayed neutron fraction β_{eff} using in-pile reactivity oscillations and Fourier analysis is presented. This method is based on measurements of the reactor's power response to small periodic in-pile reactivity perturbations and utilizes Fourier analysis for reconstruction of the reactor zero power transfer function. This approach enables the estimation of β_{eff} using multi-parameter nonlinear weighted least-squares fit. The method extends previous works by accounting for higher harmonics excitation in the frequency domain by the trapezoidal reactivity signal, both in the reactivity perturbation and in the reactor power response. We show that by using this new approach it is possible to obtain the reactor transfer function in a wide range of frequencies, using only a single oscillation frequency. This method is applied to a set of measurements of the MAESTRO core configuration in the MINERVE zero power reactor (ZPR) located at the Cadarache Research Center. The derived value of β_{eff}, using this method, is 711 ± 17 pcm.

Keywords: effective delayed neutron fraction; reactor kinetics; response function; reactor safety; critical experiment; reactor physics

1. Introduction

Delayed neutrons are of fundamental importance in the field of nuclear reactor dynamics and control. Although only a small fraction of the neutrons emitted by fission are not prompt, the knowledge of the delayed neutron parameters is essential for transient analysis, such as startup or shutdown of the reactor, as well as for accident analysis and control system design [1].

A well-known model frequently implemented in the study of nuclear reactor dynamics is the point reactor model. In the context of this model, the delayed neutron characteristics are lumped in several representative groups of constant parameters which adequately describe the time dependence of the delayed neutron precursors [2]. One of the main delayed neutron parameters used in the point reactor model equations is the effective delayed neutron fraction β_{eff}, which incorporates both delayed neutron spectral properties and core geometrical configuration [1,2]. Additional delayed neutron parameters include the fraction of fission neutrons emitted in each delayed group β_j and the delayed neutron precursors decay constants λ_j.

Experimental efforts aimed at determining the value of β_{eff}, which provide experimental support for the evaluation of delayed neutron parameters, are extremely valuable. This is due to the fact that unlike other fields in reactor physics, e.g. criticality safety or shielding, the availability of experimental data and benchmark problems for validating delayed neutron parameters and its implementation in different models is highly limited [3,4]. Furthermore, the existing experimental data exhibit significant discrepancies between the different sets of parameters [5], which lead to substantial disparity in the analysis of kinetic experiments and reactor dynamic behavior [4,6–8].

The small number of experiments dedicated to the evaluation of β_{eff}, along with the significant discrepancies between the delayed neutron parameter sets, strongly emphasize the need for novel and more accurate experiments aimed at measuring this value in thermal

*Corresponding author. Email: gilade@bgu.ac.il

reactors [4,9]. According to the WPEC Subgroup 6 report [9], the utilization of critical facilities for in-pile measurements designed for validating the calculations of thermal reactors is recommended. In addition, the WPEC Subgroup 6 report recommends a target accuracy of 3% for β_{eff} calculations, which imposes an upper limit on the uncertainty associated with experiments in order for them to be useful for nuclear data validation [4,9]. The analysis of the MISTRAL experiments on the effective delayed fraction β_{eff} in the EOLE zero power reactor (ZPR) [10], for UO_2 and MOX LWR cores, performed using noise techniques and the European nuclear data file JEFF-3.1.1, led to very satisfactory results with C/E within uncertainty limits of 1.6% (1σ).

In this work, a method for determining the effective delayed neutron fraction β_{eff} using in-pile reactivity oscillation and Fourier analysis is presented. The method is based on measurements of the reactor's power response to small periodic in-pile reactivity perturbations and utilizes Fourier analysis for reconstruction of the reactor zero power transfer function. Knowledge of the reactor transfer function enables the estimation of β_{eff} using a fitting procedure.

The method presented here extends a previous work by Yedvab et al. [4] in which the delayed neutron normalized emission rate (NER) is evaluated in the frequency domain using in-pile reactivity oscillations. While Yedvab et al. [4] observed excitation of higher odd harmonics in the frequency domain triggered by the trapezoidal reactivity signal; they did not account for it in their analysis. In this work, we account for these higher harmonics, both in the reactivity perturbation and in the power response, showing that it is possible to reconstruct the reactor transfer function (or the delayed neutrons emission rate) over a wide range of frequencies using only a single oscillation at a low frequency.

2. Theoretical background

2.1. *Derivation of the transfer function*

Study of the reactor power level response to small reactivity perturbations is of great importance regarding the stability and control of the reactor. The reactor power level response is described by a transfer function, which summarizes the main physical parameters controlling the reactor's dynamics [1,2,10,11]. For a critical reactor operating at low power (such that the reactivity is not affected by the reactor's power level), the relation between small reactivity perturbation and the consequent small power response is derived by linearization of the point reactor dynamic equations [1,2,10,11] expressed by

$$\delta P(s) = \delta\rho(s)\, P_0\, R(s), \tag{1}$$

where $\delta\rho(s)$ is the Laplace transform of small reactivity perturbation $\delta\rho(t)$, $\delta P(s)$ is the Laplace transform of the consequent small power response $\delta P(t)$, P_0 stands for the mean power, s is a complex variable, and $R(s)$ is the zero power transfer function given by

$$R(s) = \frac{1}{P_0}\frac{\delta P(s)}{\delta\rho(s)} = \left(s\Lambda + \sum_j \frac{s\beta_j}{s+\lambda_j}\right)^{-1}. \tag{2}$$

Thus, the transfer function formula encapsulates the point reactor model dynamic parameters: Λ, β_j, and λ_j. Note that the transfer function $R(s)$ is complex and its explicit representation in the frequency domain $R(i\omega)$ is obtained by substituting $i\omega$ for s [1,10,11]. For $s\sim\lambda_j$ and $\Lambda\sim10^{-5}$ seconds, the $s\Lambda$ term can be neglected since $\Lambda \ll \beta_j/(s+\lambda_j)$ and Equation (2) becomes

$$R(s) \xrightarrow{s\sim\lambda_j} \left(\sum_j \frac{s\beta_j}{s+\lambda_j}\right)^{-1}. \tag{3}$$

Once the transfer function $R(i\omega)$ is measured over a range of frequencies it is possible to apply a fit procedure to determine the required delayed neutron parameters. For example, it is customary to assume that the delayed precursors group decay constants λ_j are known and determine the β_j through the fit procedure. Actually, it is enough to measure the transfer function amplitude $|R(i\omega)|$ for the fit procedure, disregarding its phase.

2.2. *Measurement of the transfer function*

A simple procedure for measuring the reactor transfer function is to periodically perturb a low power critical reactor by in-pile oscillations of a small reactivity sample and monitor both the position of the sample and the power level as a function of time. The reactivity perturbation may be applied using a control rod or a mechanical piston able to insert small samples into the core. The appropriate transforms should then be applied to both signals and the transfer function can be obtained.

This procedure requires fine tuning of the reactivity perturbation amplitude $\delta\rho$. On one hand, the perturbation should be large enough in order to overcome the inherent stochastic fluctuations characterizing the neutron flux and the acquisition system in the reactor. On the other hand, the perturbation should be small enough such that the linearization of the point reactor model equations is not invalidated. More specifically, the method for determining the transfer function values is as follows. For a pure sinusoidal perturbation with a distinct frequency ω_0, e.g.

$$\delta\rho(t) = \delta\rho_0 \sin(\omega_0 t), \tag{4}$$

where $\delta\rho_0$ is a constant reactivity worth of the perturbation, the reactor power response as a function of time is [1,11]

$$\delta P(t) = P_0 \delta\rho_0\, |R(i\omega_0)| \sin(\omega_0 t + \phi), \tag{5}$$

where ϕ is the transfer function phase angle. Since $\delta P(t)$ is periodic it can be represented by a sum of its Fourier modes,

$$\delta P(t) = \int_{-\infty}^{\infty} \delta \tilde{P}(\omega) \sin(\omega t) d\omega. \tag{6}$$

In this case, the only non-zero Fourier component of $\delta P(t)$ is

$$\delta \tilde{P}(\omega_0) = P_0 \delta\rho_0 \left| R(i\omega_0) \right|. \tag{7}$$

In order to determine the transfer function amplitude $|R(i\omega)|$ and discard the phase contribution, the modulus is taken for both sides of Equation (7) to obtain

$$P_0 \left| R(i\omega_0) \right| = \frac{\left| \delta \tilde{P}(\omega_0) \right|}{|\delta\rho_0|}. \tag{8}$$

Generalizing the above result, any arbitrary periodic perturbation waveform $\delta\rho(t)$ can be decomposed into its Fourier components:

$$\delta\rho(t) = \int_{-\infty}^{\infty} \delta\tilde{\rho}(\omega) e^{i\omega t} d\omega. \tag{9}$$

Each Fourier component of the reactivity perturbation is transformed independently into a corresponding component in the power response of the reactor [11]:

$$\begin{aligned} \delta P(t) &= \int_{-\infty}^{\infty} \delta \tilde{P}(\omega) e^{i\omega t} d\omega \\ &= P_0 \int_{-\infty}^{\infty} \delta\tilde{\rho}(\omega) \left| R(i\omega) \right| e^{i(\omega t + \phi)} d\omega. \end{aligned} \tag{10}$$

Hence, an expression for the transfer function amplitude is obtained in the frequency domain

$$P_0 \left| R(i\omega) \right| = \frac{\left| \delta \tilde{P}(\omega) \right|}{\left| \delta\tilde{\rho}(\omega) \right|}. \tag{11}$$

Note that for the method of in-pile oscillations, the waveform of the power response signal in the time domain $\delta P(t)$ can be rather complicated, making the analysis extremely non-trivial; whereas the power response signal in frequency domain $\delta \tilde{P}(\omega)$ will show distinct maxima at the resonant frequencies ω_n making the analysis simpler.

2.3. *Pseudo-square waveform for the reactivity perturbation*

In the measurements performed in the MINERVE ZPR, the reactivity perturbation was induced by a periodic insertion of a small reactivity worth water sample using a dedicated high accuracy mechanical piston [12]. The movement of the piston was chosen to be trapezoidal, i.e. the reactivity sample position toggled between two stationary states – inside and outside the core, with a short (∼1 s) transition between them.

Unlike pure sinusoidal signal, which excites a single Fourier mode, the quasi-square signal excites a series of higher modes (harmonics) in addition to the fundamental one. For oscillations with period $T \gg 1$ second, the piston waveform signal quickly approaches the shape of a square waveform, in which case the excited higher harmonics are given by the Fourier series of a square signal:

$$\begin{aligned} \delta\rho(t) &= \sum_{n=0}^{\infty} \rho_n \sin(\omega_n t) \cong \rho_0 \frac{4}{\pi} \sum_{n=1,3,5,\ldots}^{\infty} \frac{\sin(\omega_n t)}{n}, \\ \omega_n &\equiv 2\pi f n, \end{aligned} \tag{12}$$

where f is the oscillation frequency of the piston and ρ_0 is the reactivity worth of the sample. An important feature of the square signal is that the energy stored in its higher harmonics decays like n^{-1}. This slow decay with n facilitates a proper signal to noise ratio of the higher harmonics excited by the reactivity perturbation. The general formula for the transfer function amplitude for each frequency ω_n is

$$P_0 \left| R(i\omega_n) \right| = \frac{\left| \delta \tilde{P}(\omega_n) \right|}{\left| \delta\tilde{\rho}(\omega_n) \right|}, \tag{13}$$

where $|\delta \tilde{P}(\omega_n)|$ and $|\delta\tilde{\rho}(\omega_n)|$ are the amplitude of the Fourier components at ω_n of the power response and the reactivity perturbation, respectively.

3. Experimental setup

The oscillation experiments were performed at the MINERVE ZPR located at the CEA Cadarache Research Center. MINERVE is a pool-type (∼120 m^3) reactor operating at a maximum power of 100 W with a corresponding thermal flux of 10^9 n $cm^{-2}s^{-1}$ [13]. The core is submerged under 3 meters of water and is cooled through natural convection. The core is composed of a driver zone, which includes 40 standard highly enriched MTR-type metallic uranium alloy plate assemblies surrounded by a graphite reflector. An experimental cavity (70 × 70 cm), in which various UO_2 or MOX cladded fuel pins can be loaded in different lattices, reproducing various neutron spectra [13,14], is located in the center of the driver zone. An oscillator piston, capable of moving periodically and vertically between two positions located inside and outside of the core is located inside the experimental zone. A general view of the MINERVE reactor is shown in **Figure 1**, together with schematic drawings of the reactor geometrical configuration and the MAESTRO core configuration [15].

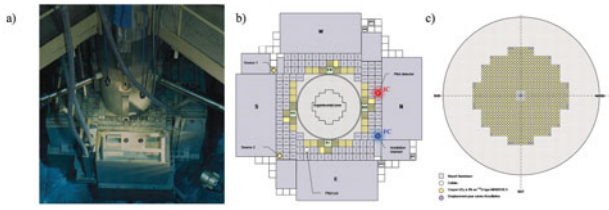

Figure 1. Schematics of the MINERVE reactor. (a) General view of the reactor [13]. (b) Schematic drawing of the MINERVE reactor structure [14]. (c) Schematic drawing of the MAESTRO core configuration [15]. The location of the IC and FC detectors is marked by red and blue circles, respectively, in panel (b).

Our measurements at MINERVE lasted 6 days using the MAESTRO core configuration [14,15]. The experiment was performed using 16 different oscillation frequencies in the range 0.005 to 0.25 Hz, with 100 full period cycles obtained for most frequencies. The average power level during the measurements was approximately 10 W, with maximal power oscillation of $\pm 2\%$ and an average power level drift of less than 1% per minute. The reactivity oscillations were introduced into the reactor using a dedicated mechanical piston, mounted with a light water sample. The water sample acted as an additional moderator, which introduced an additional reactivity of 3.79 ± 0.02 pcm into the core [16].

The neutron count rate was measured using three thermal neutron detectors: ^{10}B based ionization chamber (IC), high sensitivity (CF8R, 8 mm diameter, 1.6 mg fissile material deposit) fission chamber (FC) and a low sensitivity (CF3R, 3 mm diameter, 20 μg fissile material deposit) FC [17]. The IC was operated in current mode, avoiding dead time corrections that originated from the detector's high neutron sensitivity, whereas both FCs operated in pulse mode. The typical count rate in the CF8R detector was 2000 cps, and hence no dead time correction was required with an average dead time constant of $\sim$0.5 μs. The detectors location is marked in Figure 1(b) by red (IC) and blue (FC) circles (next to the north side of the core).

The detectors outputs, along with a trigger signal used for synchronizing the piston position and the detectors acquisition, were recorded using two PC-based Fast Comtec acquisition cards (model MCA-3FADC),[1] with a counting time per channel (time resolution Δt) of 0.1 s. This Δt was chosen such that it offered an appropriate number of channels for the entire frequency range sampled in the experiment (4000 channels for the highest oscillation frequency of 0.25 Hz and 256,000 channels for the lowest frequency 0.005 Hz).

4. Results and data analysis

An example of the reactivity perturbation worth (proportional to the piston's position) and the corresponding IC and the more sensitive FC signals (total neutron count) for a 60 s oscillation period is shown in

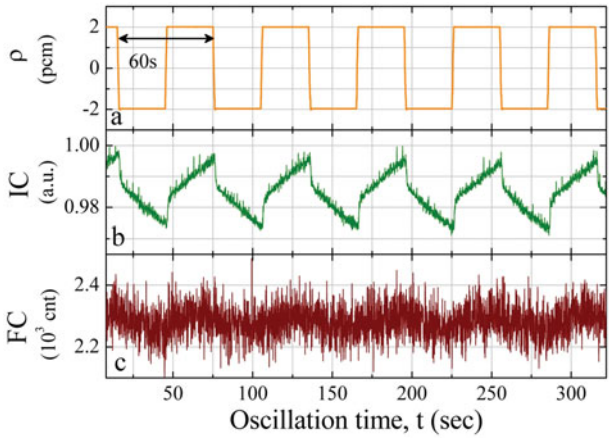

Figure 2. The temporal dynamics of the external reactivity perturbation, introduced by the oscillating piston (a) and the corresponding IC and FC counts (b and c, respectively), obtained for a 60 s oscillation period.

Figure 2. The prompt response of the neutron flux to the piston movement, as well as the delayed neutron dynamics, can be clearly observed. The sharp trapezoidal (nearly square) waveform of the reactivity perturbation is also evident (Figure 2(a)). The statistical precision of the IC is significantly higher than that of the FC (Figure 2(b) and 2(c)). Hence, the power oscillations observed by the FC are obscured by statistical fluctuations, which limit the derived number of higher harmonics (see Section 4.2). The sharp upward "spikes" visible in the IC signal (Figure 2(b)) originate from the voltage to frequency converter. Although these "spikes" add positive counts, they are sharp, their occurrence is infrequent and their effect on the power spectrum is negligible.

4.1. Experimental error estimation

There are three main independent contributions for the experimental error associated with the transfer function amplitude measurements. The first contribution, marked by σ_{drift}, is due to the drift in the reactor power level during the oscillations. The second one, marked by σ_{stat}, is due to statistical fluctuations characterizing the neutron flux, the detectors response, and the electronic acquisition system. The last one, marked by σ_{react}, stems from the uncertainty in the reactivity worth of the induced perturbation. These errors are estimated for each value of the transfer function, i.e. for each harmonic value for each oscillation period. Assuming the errors are independent, the total uncertainty (1σ) for each value is estimated according to

$$\sigma_{\text{total}} = \sqrt{\sigma_{\text{stat}}^2 + \sigma_{\text{drift}}^2 + \sigma_{\text{react}}^2}. \qquad (14)$$

During the measurements campaign, the MINERVE automatic pilot rod, which is usually used to compensate for reactivity changes due to samples oscillations, was disconnected and the power level was regulated

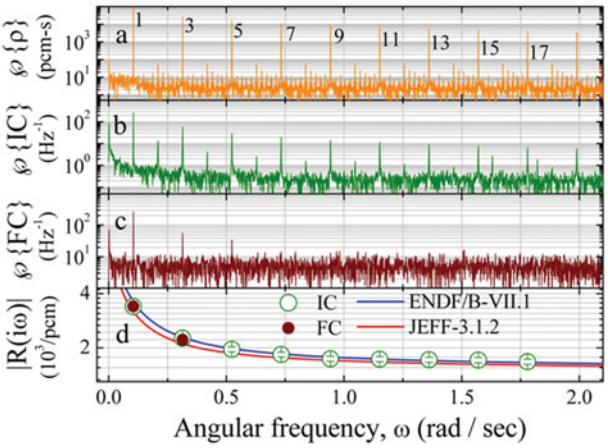

Figure 3. The obtained transfer function amplitude, $|R(i\omega)|$, calculated for an oscillation period of 60 s. (a) The reactivity perturbation power spectrum. (b) The IC detector signal power spectrum. (c) The FC detector signal power spectrum. (d) The resulting transfer function amplitude values alongside curves obtained by substituting the delayed group constants from ENDF/B-VII.1 and JEFF-3.1.2 neutron data libraries into Equation (3), using $\beta_{\text{eff}} = 650$ and 665 pcm, respectively.

manually using a control rod. Generally, the power level of the reactor was stabilized around 10 W and the reactor was critical prior to the oscillations startup. In some cases, the reactor was slightly off-critical at startup, leading to slow and steady power drift during the oscillations. In most cases, the drift was extremely mild (less than 1% per minute) and in other cases it was compensated manually during the measurement. The propagated uncertainty in the power spectrum harmonic height (**Figure 3**(b) and 3(c)) is estimated by correcting the experimental results. This drift removal was obtained using moving window averaging. The uncertainty is estimated for each harmonic for each oscillation period and is found to be more pronounced for higher frequencies. Its average value is $\sigma_{\text{drift}} \sim 2\%$ for the IC detector and $\sigma_{\text{drift}} \sim 1\%$ for the FC detector.

The statistical error originates from the statistical variance characterizing the neutron population in the reactor, the detector response, and the fluctuations in the electronic acquisition system. The standard deviation of the IC and FC detectors counts is estimated for each measurement according to $\sigma_{\text{stat}} = \text{std}(y_i - y_{i-1})$, $i = 2, \ldots, N$, where y_i is the detector count at t_i and N is the total number of sample points. This conservative approach assumes that the time-scale characterizing the statistical variations is significantly shorter than that of the power oscillations (Figure 2(b)). Hence, the obtained σ_{stat} is slightly overestimated. The propagation of this statistical variance to uncertainty in the power spectrum harmonics height is estimated using a Monte Carlo resampling technique [18]. In this technique, the obtained counts for each channel are varied by adding normally distributed random noise, generated with the appropriate standard deviations. The new varied data is analyzed and the new power spectrum harmonics are derived. This procedure is repeated (~500) and a histogram of the harmonic heights is obtained. The standard deviation of this histogram represents the propagated counting errors. This uncertainty is found to be larger for higher frequencies and its average value is ~1%.

The uncertainty in the reactivity worth of the induced perturbation is estimated using measurements performed without the water sample mounted on the oscillator (time periods of 4 s, 30 s, 60 s and 120 s were measured). The accumulated reactivity worth of both the water sample and the aluminum rod was estimated to be 4.02 ± 0.06 pcm (1σ).

4.2. *Determine the transfer function amplitude*

In order to determine the transfer function amplitude we apply Fourier transform to both the reactivity perturbation and the power response signals according to Equation (11). An example of the 60 s oscillation period analysis is shown in Figure 3, where the reactivity perturbation (Figure 3(a)), the power spectrum harmonics, obtained by the IC and FC detectors (Figure 3(b) and 3(c)) and the derived transfer function amplitude (Figure 3(d)) are plotted in the frequency domain. The fundamental mode and the higher harmonics are obtained at $\omega_n = 2\pi n/60$ rad/s for odd n.

The ratio between the harmonics height and the noise decreases and the uncertainty in the derived harmonic heights increases with the harmonic's order n. Hence, the number of harmonics used in each oscillation period is chosen according to a threshold based on the harmonics height to noise ratio. The transfer function amplitude values of the 60 s period measurement, corresponding to the first 9 harmonics with the threshold set at $n = 17$, are shown in Figure 3(d), along with curves obtained by substituting the delayed group constants from ENDF/B-VII.1 [19] and JEFF-3.1.2 [20] neutron data libraries into Equation (3), using $\beta_{\text{eff}} = 650$ and 665 pcm, respectively. In all measurements, the number of harmonics obtained from the FC count is significantly smaller than that obtained using the IC count, due to the large statistical uncertainty in the former (see Section 4.1).

The obtained values of $|R(i\omega)|$ using all oscillation periods with their respective harmonics are presented in **Figure 4**. Also presented are calculated curves (according to Equation (3)) using available neutron data library. In addition, the calculated curve based on the neutron data derived in the present work is plotted (see Section 4.3). This curve exhibits good qualitative agreement with those of the literature (Figure 4).

4.3. *Estimation of the delayed neutron fraction β_{eff}*

The data points of the transfer function amplitude, obtained using both the IC and FC, were used to fit

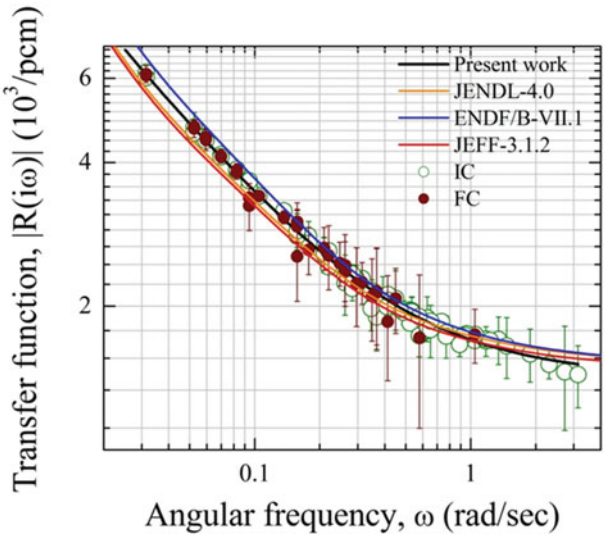

Figure 4. The obtained values of $|R(i\omega)|$ using the IC (open) and the FC (closed), including all oscillation periods and their higher harmonics, as a function of angular frequency. Also presented are theoretical curves (Equation (3)) of the transfer functions, using the neutron data libraries ENDF/B-VII.1 (blue), JEFF-3.1.2 (red), and JENDL-4.0 (orange). In addition, the calculated curve based on the neutron data derived in the present work is presented (black). The error bars correspond to 1σ.

curves of the theoretical form described in Equation (3). The fitting procedure was applied using multi-parameter nonlinear weighted least-squares fit, where for each library, the delayed neutron precursors decay constants λ_j were fixed, s was an independent variable, the data points were the dependent variables, the delayed neutron group yield β_j were the fitted parameters, the β_j from the library were used as an initial point, and the inverse of the errors were used as weights. The available neutron data libraries used for the fitting procedure are specified in **Table 1**. The differences between the obtained transfer functions were negligible, indicating small sensitivity of the fitting procedure to a specific choice of the neutron data library. Note that in the case of the JEFF-3.1 and ROSFOND libraries, eight groups of delayed neutron decay constants were used, whereas six groups were used for the other libraries. The decay constants used are of ^{235}U thermal fission.

The effective delayed neutron fraction is calculated according to $\beta_{\text{eff}} = \sum_j \beta_j$ for each library. The uncertainty in β_{eff} results from (1) the propagation of the statistical errors $\Delta\beta_{\text{stat}}$, (2) the propagation of uncertainty in the induced reactivity perturbation $\Delta\beta_{\text{react}}$, and (3) the propagation of uncertainty in the λ_j sets taken from different libraries.

The statistical errors in the transfer function values are propagated to $\Delta\beta_{\text{stat}}$ by applying a Monte Carlo resampling technique (see Section 4.1). Each value of the obtained transfer function (Figure 4) is varied by adding normally distributed random noise with standard deviation of $\sigma = \sqrt{\sigma_{\text{stat}}^2 + \sigma_{\text{drift}}^2}$.

The uncertainty in the induced reactivity perturbation $\Delta\beta_{\text{react}}$ results from uncertainty in the sample reactivity worth and the reactivity contribution of the piston itself. In principle, the reactivity contribution of the piston itself (without a water sample) should be negligible, since the inside and outside piston states should induce similar reactivity perturbations. However, power oscillations were detected in response to "piston-only" oscillation experiments. Analysis of these experiments yields a piston's reactivity worth of 0.23 ± 0.05 pcm. Detailed description will be published elsewhere. Thus, the total reactivity worth of the induced perturbation is 4.02 ± 0.06 pcm. Finally, the uncertainty in the induced reactivity perturbation is propagated to $\Delta\beta_{\text{react}} = 11$ pcm.

A value of β_{eff} is obtained for each λ_j set (taken from different neutron data libraries). The uncertainty in the λ_j sets is propagated to an uncertainty in β_{eff} by evaluating the standard deviation of the different β_{eff} values (Table 1). Although underestimated due to the existence of correlations between the different λ_j sets, this uncertainty ($\sim$0.5%) is negligible compared to both $\Delta\beta_{\text{stat}}$ and $\Delta\beta_{\text{react}}$.

Table 1. Values of the effective delayed neutron fraction β_{eff} obtained for the measured transfer function data points using multi-parameter nonlinear weighted least-squares fit and delayed neutron precursors decay constants from different neutron cross section data libraries.

Library	β_{eff} (pcm)	$\Delta\beta_{\text{stat}}$ (pcm)	$\Delta\beta_{\text{react}}$ (pcm)	$\Delta\beta_{\text{eff}}$ (%)	C/E
Keepin [2]	710 ± 22	11	11	2.2	1.00857
ENDF/B-VI [22]	711 ± 22	11	11	2.2	1.00647
ENDF/B-VII [19]	711 ± 23	12	11	2.3	1.00678
JEFF-2.2 [23]	713 ± 23	12	11	2.3	1.00468
JEFF-3.1.2 [20]	708 ± 25	15	11	2.5	1.01169
CENDL-3.1 [24]	711 ± 20	10	11	2.0	1.00707
JENDL-4.0 [25]	711 ± 25	14	11	2.5	1.00708
ROSFOND [26]	709 ± 24	14	11	2.4	1.01003
Brady [27]	712 ± 22	11	11	2.1	1.00528
Tuttle [28]	713 ± 28	17	11	2.8	1.00380
Average	711 ± 17	13	11	2.3	1.00715

Assuming these uncertainties are uncorrelated, the total uncertainty in the derived value of β_{eff} is $\Delta\beta = \sqrt{\Delta\beta^2_{\text{stat}} + \Delta\beta^2_{\text{react}}} = 17\text{pcm}$, where $\Delta\beta_{\text{stat}}$ and $\Delta\beta_{\text{react}}$ are averaged over the different libraries (see Table 1). Hence, the obtained value of β_{eff} is 711 ± 17 pcm (1σ). Recent calculations performed by CEA using TRIPOLI4.9 and JEFF-3.1.1 suggest a value of 748.8 ± 0.4 pcm (without full uncertainty analysis) and will be reported elsewhere [21].

5. Conclusions

A method for determining the effective delayed neutron fraction β_{eff} using in-pile oscillations and Fourier analysis is presented. The method developed in this work extends previous works by accounting for the higher harmonics excitation by the non-sinusoidal reactivity perturbation waveform. This work demonstrates that although previously overlooked, these higher harmonics store valuable information regarding the reactor transfer function. Furthermore, it is shown that the transfer function can be reconstructed with satisfactory precision over a wide range of frequencies using non-sinusoidal perturbation and a single oscillation frequency. The method is applied to a set of in-pile measurements performed at the MINERVE ZPR in order to determine the value of β_{eff} for the MAESTRO core configuration. This goal is achieved by applying multiparameter nonlinear weighted least-squares fit to the measured reactor transfer function using precursors decay constants from several neutron cross section data libraries [2,19,20,22–28].

The obtained value of β_{eff} is 711 ± 17 pcm (1σ) and the uncertainties associated with this result and with results obtained for each specific neutron data library (see Table 1) are small enough so that the method presented in this work can be regarded as a qualified technique for this kind of measurements [3]. Moreover, since the uncertainty, $\Delta\beta_{\text{eff}}$= 2.3%, is small enough to meet the target accuracy of 3% for β_{eff} calculations [9], the obtained values of β_{eff} can be considered as benchmarks to validate calculation methods and related nuclear data libraries used for β_{eff} determination. In this respect, the uncertainty in the applied reactivity perturbation plays a significant role and is propagated directly to an uncertainty in the value of β_{eff}. Reducing this uncertainty (which is 1.5% in this work) in this kind of experiments is of upmost importance.

A major concern in in-pile kinetic measurements is the accuracy estimation and reduction of the associated uncertainties. More specifically, the uncertainties in the present work, e.g. reactivity perturbation worth, can be reduced by performing additional measurements and by comparison to independent in-pile methods (e.g. noise techniques). These uncertainties can also be better quantified by further development of the experimental technique described in this work. Further work should, therefore, include the use of additional samples for reactivity perturbation, suppression of the power drift during the oscillations, and comparison with independent static techniques (e.g. CPSD).

Disclosure statement

No potential conflict of interest was reported by the authors.

Note

1. http://www.fastcomtec.com/?id=212

References

[1] Bell GI, Glasstone S. Nuclear reactor theory. New York: Van Nostrand Reinhold; 1970.
[2] Keepin GR. Physics of nuclear kinetics. Reading (MA): Addison-Wesley; 1965.
[3] dos Santos A, Diniz R, Fanaro LCCB, Jerez R, Silva GSA, Yamaguchi M. A proposal of a benchmark for β_{eff}, $\beta_{\text{eff}}/\Lambda$, and Λ of thermal reactors fueled with slightly enriched uranium. Ann Nucl Energy. 2006;33:848–855.
[4] Yedvab Y, Reiss I, Bettan M, Harari R, Grober A, Ettedgui H, Caspi EN. Determination of delayed neutrons source by in-pile oscillation measurements. Proceedings of PHYSOR-2006; 2006 Sep 10–14; Vancouver (Canada); 2006.
[5] Spriggs GD, Campbell JM. A summary of measured delayed neutron group parameters. Prog Nucl Energy. 2002;41:145–201.
[6] Williams T. On the choice of delayed neutron parameters for the analysis of kinetic experiments in 235U systems. Ann Nucl Energy. 1996;23:1261–1265.
[7] Svarny J. Application of different delayed neutrons data sets to the analysis of rod drop experiments on VVER cores. Prog Nucl Energy. 2002;41:303–315.
[8] Geslot B, Jammes C, Gall B. Influence of the delayed neutron group parameters on reactivity estimation by rod drop analysis. Ann Nucl Energy. 2007;34:652–660.
[9] Rudstam G, Finck Ph, Filip A, D'Angelo A. Delayed neutron data for the major actinides. Paris: Nuclear Energy Agency; 2002. (Report no. NEA/WPEC-6).
[10] Santamarina A, Blaise P, Erradi L, Fougeras P. Calculation of LWR β_{eff} kinetic parameters: validation on the MISTRAL experimental program. Ann Nucl Energy. 2012;48:51–59.
[11] Hetrick DL. Dynamics of nuclear reactors. Chicago (IL): University of Chicago Press; 1971.
[12] Antony M, Di-Salvo J, Pepino A, Bosq JC, Bernard D, Leconte P, Hudelot JP, Lyoussi A. Oscillation experiments techniques in CEA MINERVE experimental reactor. Proceedings of the International Conference on Advancements in Nuclear Instrumentation Measurement Methods and their Applications (ANIMMA); 2009 Jun 7–10; Marseille (France); 2009.
[13] Cacuci DG. Handbook of nuclear engineering. Boston (MA): Springer-Verlag; 2010.
[14] Hudelot JP, Klann R, Fougeras P, Genin X, Drin N, Donnet L. OSMOSE: an experimental program for the qualification of integral cross sections of actinides. Proceedingsof PHYSOR-2004; 2004 Apr 25–29; Chicago (IL); 2004.
[15] Leconte P, Geslot B, Gruel A, Pepino A, Derriennic M, Di-Salvo J, Antony M, Eschbach R, Cathalau S.

MAESTRO: An ambitious experimental programme in the MINERVE reactor for the improvement of nuclear data of structural, detection, absorbing and moderating materials. Proceedings of the International Conference on Advancements in Nuclear Instrumentation Measurement Methods and their Applications (ANIMMA); 2013 Jun 23–27; Marseille (France); 2013.
[16] CEA, private communication.
[17] Geslot B, Berhouet F, Oriol L, Bréaud S, Jammes C, Filliatre P, Villard JF. Development and manufacturing of special fission chambers for in-core measurement requirements in nuclear reactors. Proceedings of the International Conference on Advancements in Nuclear Instrumentation Measurement Methods and their Applications (ANIMMA); 2009 Jun 7–10; Marseille (France); 2009.
[18] Roe BP. Probability and statistics in experimental physics. New York: Springer-Verlag; 1992.
[19] Chadwick MB, Herman M, Obložinský P, Dunn ME, Danon Y, Kahler AC, Smith DL, Pritychenko B, Arbanas G, Arcilla R, Brewer R, Brown DA, Capote R, Carlson AD, Cho YS, Derrien H, Guber K, Hale GM, Hoblit S, Holloway S, Johnson TD, Kawano T, Kiedrowski BC, Kim H, Kunieda S, Larson NM, Leal L, Lestone JP, Little RC, McCutchan EA, MacFarlane RE, MacInnes M, Mattoon CM, McKnight RD, Mughabghab SF, Nobre GPA, Palmiotti G, Palumbo A, Pigni MT, Pronyaev VG, Sayer RO, Sonzogni AA, Summers NC, Talou P, Thompson IJ, Trkov A, Vogt RL, van der Marck SC, Wallner A, White MC, Wiarda D, Young PG. ENDF/B-VII.1: nuclear data for science and technology: cross sections, covariances, fission product yields and decay data. Nucl Data Sheets. 2011;112:2887–3152.
[20] JEFF-3.1.2: general purpose library for incident neutron data [Internet]. Paris (France): OECD/NEA Data Bank. Available from: http://www.oecd-nea.org/dbforms/data/eva/evatapes/jeff_31/JEFF312/.
[21] Geslot B, Pepino A, Gruel A, Di Salvo J, de Izarra G, Jammes C, Destouches C, Blaise P. Pile noise experiment in MINERVE reactor to estimate kinetic parameters using various data processing methods. Proceedings of the International Conference on Advancements in Nuclear Instrumentation Measurement Methods and their Applications (ANIMMA); 2015 Apr 20–24; Lisbon (Portugal); 2009.
[22] McLane V. ENDF/B-VI summary documentation supplement I. Upton (NY): National Nuclear Data Center, Brookhaven National Laboratory; 1996. (Report No. BNL-NCS-17541, 4th ed).
[23] The JEF-2.2 Nuclear Data Library, JEFF Report 17. OECD/NEA Data Bank; 2000.
[24] Ge ZG, Zhao ZX, Xia HH, Zhuang YX, Liu TJ, Zhang JS, Wu HC. The updated version of Chinese evaluated nuclear data library (CENDL-3.1). J Korean Phys Soc. 2011;59:1052–1056.
[25] Shibata K, Iwamoto O, Nakagawa T, Iwamoto N, Ichihara A, Kunieda S, Chiba S, Furutaka K, Otuka N, Ohasawa T, Murata T, Matsunobu H, Zukeran A, Kamada S, Katakura JI. JENDL-4.0: anew library for nuclear science and engineering. J Nucl Sci Technol. 2011; 48:1–30.
[26] Zabrodskaya SV, Ignatyuk AV, Koshcheev VN, Nikolaev MN, Pronyaev VG. ROSFOND – Russian national neutron data library. VANT Nucl Const. 2007;1–2:3–48.
[27] Brady MC, England TR. Delayed neutron data and group parameters for 43 fissioning systems. Nucl Sci Eng. 1989;103:129–149.
[28] Tuttle RJ. Delayed-neutron data for reactor physics analysis. Nucl Sci Eng. 1975;56:37–71.